

## Alternative principle and method in x-ray diagnostics for plasma electron temperatures

J. Kohagura, T. Cho, M. Hirata, T. Tamano, K. Yatsu, and S. Miyoshi  
*Plasma Research Centre, University of Tsukuba, Tsukuba, Ibaraki 305, Japan*  
 (Received 5 March 1997; revised manuscript received 14 July 1997)

An alternative principle and method in x-ray diagnostics is proposed for measurements of plasma electron temperatures  $T_e$ . The method is different from widely utilized standard methods of x-ray pulse-height analysis and x-ray absorption. This proposal is based on three-dimensionally diffusing charges produced by x rays in a field-free substrate of a semiconductor detector, although these charges have been ignored for the x-ray measurements. This proposed theory corrects the standard conventional theory on a semiconductor response employed over the past quarter of the century for  $T_e$  analyses. Overestimations of  $T_e$  and misinterpretations of broader  $T_e$  profiles may result when the conventional theory is utilized. These lead to misunderstandings of pedestal structures in high confinement modes, electron-energy transport, as well as the misestimation of bootstrap currents and hence the misinterpretations of plasma physics itself. The proposed theory is extended to construct an alternative method for  $T_e$  measurements; this method is based on detection of the diffusion-charge distributions using a semiconductor depletion layer as a temporally changeable x-ray “absorber” during one plasma shot, in place of the conventional use of the depletion layer as an x-ray-sensitive region. X-ray signals in the conventional methods have a complicated dependence on plasma densities and  $T_e$ , while the proposed method is conveniently characterized by no effects of plasma densities on the signal analyses as well as no need of complicated systems for x-ray diagnostics. This method would be useful not only for providing a practical alternative but also for clarifying the physics essentials in the proposed theory through such practical examples. [S1063-651X(97)03711-2]

PACS number(s): 52.70.La

### I. INTRODUCTION

Recently, we proposed a generalized theory on the x-ray energy response of a widely utilized semiconductor detector [1–3]. The theory solved a serious problem of a recent finding of the invalidity of the conventional standard theory [4] on the response of such an x-ray detector. The conventional theory has been utilized widely over the past quarter of the century [4] in various research fields including plasma-electron investigations. After the successful application of semiconductor detectors to plasma x-ray diagnostics [5], various uses of semiconductor detectors have been carried out in most plasma confinement devices as standard x-ray detectors. In addition, the following recent direction of plasma x-ray diagnostics enhances the importance of the correct use of the x-ray-response theory; that is, underbiased operations for semiconductor x-ray detectors are widely employed in various plasma-confinement devices including the DIII-D [6], the JET [7,8] and the ASDEX Upgrade tokamaks [9] in order to avoid detector breakdown due to the incidence of intense fusion-produced neutrons and x rays. In such underbiased operations, it is found that the problem of the use of the conventional theory is significantly enhanced; that is, serious overestimations of plasma-electron temperatures  $T_e$  and misinterpretations of the temperature profiles (see Sec. IV) result from the use of the conventional theory. Such misunderstandings of incorrect broader electron-temperature profiles (or  $\text{grad } T_e$ ), in turn, result in misleading of fundamental plasma behavior as well as essential plasma-physics understandings, for instance, the analyses of pedestal regions for high-confinement modes (H modes) and electron-energy transport (the electron diffusivity  $\chi_e$  being proportional to  $\text{grad } T_e$ ), as well as the estimation of the amount and location

of bootstrap currents (being proportional to  $\text{grad } T_e$ ) for the possibility of steady-state tokamak operations.

In the present article, in order to overcome such serious and inevitable problems coming from both the semiconductor physics itself and the above-described semiconductor operational requirements for fusion x-ray diagnostics, we propose an alternative theory of x-ray diagnostics for the determinations of x-ray energies or  $T_e$ . This proposed theory is different from the widely utilized theory in standard methods employed over the past quarter of the century, such as the methods of x-ray absorption [10–14] and x-ray pulse-height analysis (PHA) [11–15]. These methods employ direct measurements of x-ray-produced signal charges in the semiconductor depletion layer, and the conventional theory is still misused even at this time.

Thus the present article is prepared to construct and extend our proposed theory, as well as to address and systematically summarize (i) the proposed theory along with its theoretical formula (Sec. II), (ii) the experimental verification of the proposed theory (Sec. III), and (iii) the resultant effects of the present theory on plasma-physics interpretations (Sec. IV), along with (iv) an alternative  $T_e$  measurement method so as to explain the theory through such extended examples (Sec. V) for the actual understanding of plasma physics.

### II. PROPOSED THEORY ON THE X-RAY ENERGY RESPONSE OF A SEMICONDUCTOR DETECTOR

We have recently proposed a theory on the output signals of semiconductor x-ray detectors [2] and used an approximated theoretical formula without experimental data comparison [1,3]. In this section, the exact theoretical treatment

and the extension of the above theory to the signal analyses of commonly used multichannel detectors are discussed so as to clarify the proposed theory and provide the theoretical bases for comparison with the experimental data (Sec. III).

The theory predicts the enhancement of the output signals due to x-ray-produced charges (i.e., holes or electrons) in a field-free substrate region behind the depletion layer of a detector since the signals predicted by the conventional theory [4] originate from the depletion layer alone. The essential point of our theory is the inclusion of such three-dimensional diffusion effects of x-ray-produced charges on the total signals. The importance of these x-ray-response studies is highlighted by the comparison of the significant difference in  $T_e$  deduced from the conventional theory [4] and from our formula. The problem becomes more complicated when we employ a multichannel semiconductor-detector array fabricated on one silicon wafer for the purpose of x-ray tomographic reconstructions [6–9,11–13]. In this case, the three-dimensionally diffusing charges from the field-free substrate of an x-ray injected channel to the neighboring channels behave as “channel cross talk.”

The charge diffusion effect leads us to propose an alternative idea of x-ray diagnostic methods for  $T_e$  measurements. Suppose distribution profiles of such x-ray-produced charge diffusion in a multichannel detector are observed; then the charge distributions give information about  $T_e$  because of the dependence of the distribution profile on x-ray energies or, in turn, the temperatures of the x-ray-emitting electrons. These distribution signals are characterized by the independence of plasma densities (see Sec. V). Such a property shows a significant difference from the x-ray-signal dependence of bremsstrahlung on both ion and electron densities  $n_i$  and  $n_e$ , respectively. The direct observations of such x-ray emission using the depletion layer of a semiconductor detector have been employed for the x-ray PHA and the x-ray-absorption method. Moreover, it is noteworthy that the proposed method can provide information on the spatial and temporal evolution of  $T_e$  during one plasma shot only by taking advantage of the combination of the physical characteristics of such diffusion profiles in a substrate of a multichannel semiconductor-detector array [16] with our proposed alternative use of a depletion layer as an x-ray “absorber” in place of its conventional use as an x-ray-sensitive layer (see Sec. V).

In this section, the fundamental theory is summarized for the purpose of providing a comparison between the theory and the experiments in Sec. III, as well as characterizing the present method so as to compare it with the previously established standard methods [10]. We first formulate the theory of the three-dimensional thermal diffusion of x-ray-produced charges in a semiconductor field-free substrate region. The three-dimensional diffusion equation for a charge flux  $\phi$  created in a substrate by x rays is described as

$$\frac{1}{r^2} \frac{d}{dr} r^2 \frac{d\phi(r)}{dr} - \frac{1}{L^2} \phi(r) = -\frac{s(d)}{D}, \quad (1)$$

where the minority-carrier diffusion length  $L$  is written as  $L^2 = D\tau$  and  $D$  and  $\tau$  are the diffusion coefficient and the lifetime of the charge, respectively. Here  $\tau$  ranges a few microseconds; for instance,  $D = 34\text{--}39 \text{ cm}^2/\text{s}$  for  $L = 75 \text{ }\mu\text{m}$

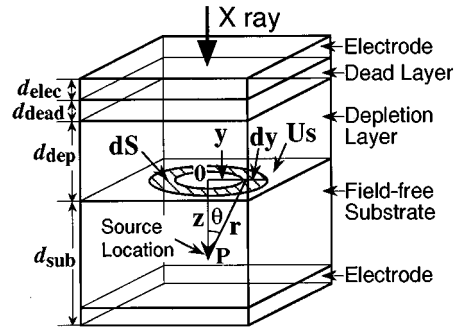


FIG. 1. Schematic view of a single-channel semiconductor x-ray detector.

and  $\tau = 1.7\text{--}1.4 \text{ }\mu\text{s}$ . If the characteristic time of the temporal variation in x-ray radiation from plasmas is sufficiently longer than  $\tau$  and intense x-ray signals are observed in a current (pileup) mode, then a quasisteady state for the charge-diffusion process is treated, as seen in Eq. (1). The source charge  $s$  is created by incident x rays at a depth of  $d$  from the front surface of the field-free substrate. The distance from the source location  $P$  in Fig. 1 to the bottom surface of the depletion layer is denoted as  $r$  (see Fig. 1). A flow density of the charge  $J(r)$  from  $P$  along  $r$  is defined as

$$J(r) = -D \frac{d\phi}{dr} = \frac{s}{4\pi r^2} \left( \frac{r}{L} + 1 \right) \exp\left( -\frac{r}{L} \right), \quad (2)$$

where

$$s(d) = I_0 \left( \frac{E}{\epsilon} \right) \mu \rho \exp(-\mu \rho d). \quad (3)$$

Here  $I_0$  is the x-ray intensity with an energy  $E$  at the front surface of the substrate (see Fig. 1) and  $\epsilon$  stands for the energy required to create an electron-hole pair. The values of  $\mu$  and  $\rho$  denote the silicon mass-absorption coefficient and the mass density, respectively.

The total amount of the three-dimensionally diffusing minority carriers from the production point  $P$  (Fig. 1) to the depletion-layer surface contributes to a signal and is described as the integral of  $\text{div } \mathbf{J}$  for the substrate volume; this integral is rewritten as the surface integral  $\int J dS$  surrounding the substrate. We then integrate over  $z$  from 0 to the thickness of the substrate  $d_{\text{sub}}$  to scan the source point  $P$  in the substrate along the x-ray path in the  $z$  direction (Fig. 1). Furthermore, the effect of the external bias circuit is described by a factor 2 multiplication of the “pure” diffusion effect. Thus the amount of the overall diffusion charges  $F_{\text{new}}$  is described as

$$F_{\text{new}} = I_0 \frac{E}{\epsilon} \mu \rho \frac{L}{\mu \rho L + 1} \left\{ 1 - \exp\left[ -\left( \mu \rho + \frac{1}{L} \right) d_{\text{sub}} \right] \right\}. \quad (4)$$

The total collection of charges  $F_{\text{total}}$  created in both a depletion layer and a field-free substrate for a single-channel detector is then described as

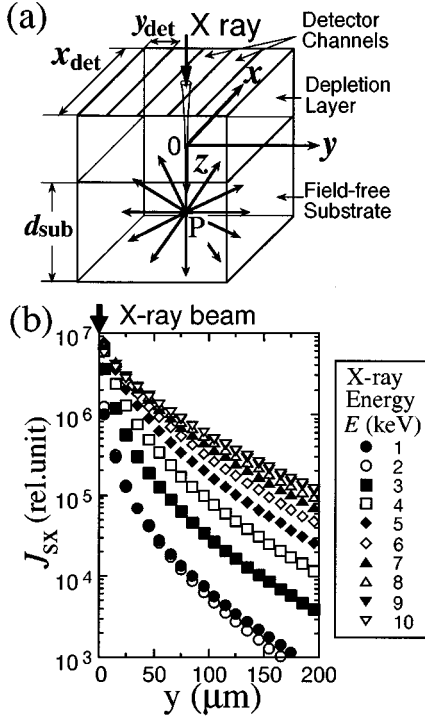


FIG. 2. (a) Schematic view of a multichannel semiconductor x-ray-detector array. (b) Theoretical results of the charge-diffusion distributions  $J_{sx}$  using Eq. (8) from a multichannel detector for unit-intensity x rays. X rays are injected at  $x=y=0$  with the energy  $E$  from 1 to 10 keV. Here the typical values of  $d_{\text{sub}}=300 \mu\text{m}$  and  $L=100 \mu\text{m}$  are utilized. Each channel size is denoted as  $x_{\text{det}}$  and  $y_{\text{det}}$ .

$$\begin{aligned}
 F_{\text{total}} &= I_{\text{plas}} \exp(-\mu_{\text{dead}} \rho_{\text{dead}} d_{\text{dead}}) \exp(-\mu_{\text{elec}} \rho_{\text{elec}} d_{\text{elec}}) \left( \frac{E}{\varepsilon} \right) \\
 &\times \left[ 1 - \exp(-\mu_{\text{dep}} \rho_{\text{dep}} d_{\text{dep}}) + \frac{\mu \rho L}{\mu \rho L + 1} \right. \\
 &\times \left. \left[ 1 - \exp\left(-\left(\mu \rho + \frac{1}{L}\right) d_{\text{sub}}\right) \right] \right] \exp(-\mu_{\text{dep}} \rho_{\text{dep}} d_{\text{dep}}). \quad (5)
 \end{aligned}$$

Here  $I_{\text{plas}}$  is the x-ray intensity from plasmas. The subscripts dead, elec, and dep denote the dead layer, the electrode, and the depletion layer, respectively.

The theoretical analysis of the three-dimensional charge-diffusion effect is investigated for a multichannel semiconductor-detector signal using our thermal diffusion model. The charge-diffusion output profile for a multichannel semiconductor-detector array is calculated (Fig. 2).

Illustrated in Fig. 2(a) is a schematic view of a multichannel semiconductor x-ray-detector array along with an illustration of charges diffusing from a point located in the field-free substrate, where the incident x rays are absorbed. X rays are injected at  $x=y=0$ .

The incident x rays are assumed to be absorbed at the point  $P$ . Charges  $s$  produced by x-ray absorption at  $P$  diffuse in every direction according to the three-dimensional diffusion equation. Charges created in the range of a diffu-

sion length  $L$  from the depletion layer reach the bottom surface of the depletion layer (i.e., the upper surface of the field-free substrate).

In Fig. 1, charges diffusing from  $P$  to an area  $dS$  with a radius of  $y$  and a width of  $dy$  are defined as  $dQ_{\text{dif}}(y)$ . Here  $dQ_{\text{dif}}(y)$  is described as

$$dQ_{\text{dif}}(y) = 2\pi y J(r) dy = y \frac{s}{2r^2} \left( \frac{r}{L} + 1 \right) \exp\left(-\frac{r}{L}\right) \frac{z}{r} dy. \quad (6)$$

For the total charge flux, since the source charges distribute along the x-ray path in the  $z$  direction, i.e.,  $s(z)$ , the summation of the total diffusion charges is required using the integration over  $s(z)$  from 0 to the thickness of the substrate  $d_{\text{sub}}$ . Then the signal profile from the field-free substrate is rewritten for a unit area along the  $y$  direction; this normalized value  $q_{\text{dif}}(y)$  is described as

$$\begin{aligned}
 q_{\text{dif}}(y) &= \frac{I_0}{4\pi} \frac{E}{\varepsilon} \mu \rho \int_{r=y}^{\sqrt{y^2+d_{\text{sub}}^2}} \frac{1}{r^2} \left( \frac{r}{L} + 1 \right) \\
 &\times \exp\left(-\frac{r}{L} - \mu \rho \sqrt{r^2 - y^2}\right) dr. \quad (7)
 \end{aligned}$$

A multichannel detector array with each channel size of  $x_{\text{det}}$  and  $y_{\text{det}}$  [Fig. 2(a)] is widely employed for x-ray tomography diagnostics. In the case of  $x_{\text{det}} \gg L$ , we integrate over  $x$  from  $x_{\text{det}}/2$  to  $-x_{\text{det}}/2$  to take account of the charge-diffusion distribution in the  $x$  direction; here  $x_{\text{det}}$  is the total width of the detector. Consequently, for the configuration of Fig. 2(a), an output-signal profile from the multichannel-detector array for unit-intensity x rays is written as

$$\begin{aligned}
 J_{sx}(y) &= \int_{x=-x_{\text{det}}/2}^{x_{\text{det}}/2} \frac{I_0}{4\pi} \frac{E}{\varepsilon} \mu \rho \int_{r=\sqrt{y^2+x^2}}^{\sqrt{y^2+x^2+d_{\text{sub}}^2}} \frac{1}{r^2} \left( \frac{r}{L} + 1 \right) \\
 &\times \exp\left(-\frac{r}{L} - \mu \rho \sqrt{r^2 - (y^2+x^2)}\right) dr dx. \quad (8)
 \end{aligned}$$

Here we define the distance  $r$  as  $r^2 = x^2 + y^2 + z^2$ .

The curves in Fig. 2(b) show the calculated diffusion signals  $J_{sx}(y)$  using our three-dimensional diffusion theory. Figure 2(b), in turn, provides an essential idea to identify the incident x-ray energy using such charge diffusion distributions. Therefore, it is important to note that the distributions, depending on the incident x-ray energy or x-ray-emitting electron temperatures, are independent of plasma densities since the densities enhance only the intensities of x-ray emission and the resulting amount of charge diffusion and they do not change the charge-distribution shapes in Fig. 2(b). This characteristic feature of the independence of the charge distributions on plasma densities is different from the dependence of commonly utilized bremsstrahlung on  $n_e n_i$  for usual plasma x-ray diagnostics. Such a density dependence of bremsstrahlung makes x-ray diagnostics complicated to distinguish  $T_e$  from the effects of plasma densities so as to determine  $T_e$ ; consequently, the proposed theory would provide the possibilities for plasma x-ray diagnostics to analyze  $T_e$  directly. A practical application method for  $T_e$  analyses

using this principle is proposed in Sec. V as the third method following the two well-established methods of the x-ray-absorption method and the x-ray PHA. The proposed theory would be clarified through such examples.

$$F_d(y) = \int_{y_{\text{sou}}=|y_{\text{sou}1}|}^{|y_{\text{sou}2}|} \int_{x=-x_{\text{det}}/2}^{x_{\text{det}}/2} \frac{I_0 E}{4\pi \varepsilon \mu \rho} \int_{r=\sqrt{(y+|y_{\text{sou}1}|)^2+x^2}}^{\sqrt{(y+|y_{\text{sou}1}|)^2+x^2+d_{\text{sub}}^2}} \frac{1}{r^2} \left( \frac{r}{L} + 1 \right) \exp\left( -\frac{r}{L} - \mu \rho \sqrt{r^2 - [(y+|y_{\text{sou}1}|)^2+x^2]} \right) dr dx dy_{\text{sou}}. \quad (9)$$

Here the width of the incident x-ray beam  $y_{\text{sou}}$ , producing source charges, is written as  $y_{\text{sou}} = y_{\text{sou}1} - y_{\text{sou}2}$ ;  $y_{\text{sou}1}$  and  $y_{\text{sou}2}$  are the locations of both edges of the rectangular x-ray beam. Equation (9) provides a more convenient formula for experiments using a finite-size x-ray beam.

### III. EXPERIMENTAL VERIFICATION OF THE THREE-DIMENSIONAL DIFFUSION EFFECT

#### A. Experimental apparatus

For the purpose of the verification of our theory of the three-dimensional diffusion of x-ray-produced charges, synchrotron radiation from a storage ring is employed as a monochromatic x-ray source. The experiments are carried out as follows. A 2.5-GeV positron storage ring having a mean diameter of 60 m at the Photon Factory in High Energy Accelerator Research Organization (KEK) provides intense synchrotron radiation [15,17]. The energy is monochromatized and automatically changed using a computer-controlled double-crystal [Si(111)] monochromator with an energy resolution of a few eV (Fig. 3). In order to suppress higher-order reflection of x rays, the crystals are deviated slightly from the parallel location. The purity of the energy is monitored using a NaI(Tl) detector. X rays ranging from 5 to 20

keV are monitored by ionization chambers using nitrogen or argon gas. This output signal (an  $I_0$  monitor signal) is converted into a frequency signal by a voltage-to-frequency converter and then the signal is counted by a scaler with 2 s of accumulation and processed by the microcomputer.

A rectangularly collimated x-ray beam ( $240 \mu\text{m} \times 3.5 \text{ mm}$ ) at 9.5 keV is incident onto a specially fabricated microstrip silicon detector having 520 channels on a  $5.2 \text{ mm} \times 5.2 \text{ mm} \times 300 \mu\text{m}$  thick silicon wafer (i.e., a  $10 \mu\text{m}$  width per channel); this detector was originally designed for the CERN Omega telescope project and modified for our physics experiments [see below; Fig. 4(a)].

A precise computer-controlled position scanner for the microstrip detector is prepared for its precise setting with

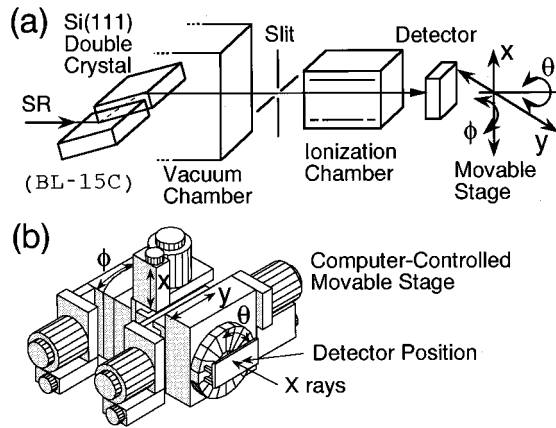


FIG. 3. (a) Schematic drawings of the experimental setup (BL15C) using synchrotron radiation at the Photon Factory in High Energy Accelerator Research Organization (KEK). (b) Computer-controlled position-adjustable system having the position resolution and reproducibilities within  $x=y=0.5 \mu\text{m}$ ,  $\theta=0.005^\circ$ , and  $\phi=0.002^\circ$ .

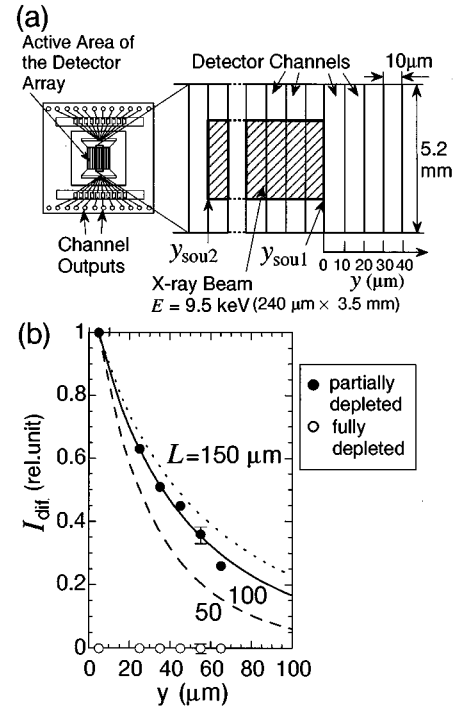


FIG. 4. (a) Schematic drawings of a modified CERN strip detector. The expanded active area of the detector and the incident x-ray-beam location are depicted along with the definition of the  $y$  coordinates. (b) Experimental data in the cases of a fully depleted and a partially depleted operation shown by the open and the filled circles, respectively; the dashed, solid, and dotted curves are calculated using our theoretical formula of Eq. (9) for  $L=50, 100,$  and  $150 \mu\text{m}$ , respectively, along with  $d_{\text{sub}}=300 \mu\text{m}$  and  $|y_{\text{sou}}|=240 \mu\text{m}$ .

respect to the incident x-ray-beam direction [Fig. 3(b)]. Reproducible position control in the  $x$ ,  $y$ , and  $\theta$  directions on the detector surface, within an accuracy of  $0.5 \mu\text{m}$ ,  $0.5 \mu\text{m}$ , and  $0.005^\circ$ , respectively, is achieved along with goniometric control within  $0.002^\circ$ .

### B. Experimental results

In Fig. 4(b), the open and filled circles show the data obtained in a fully depleted or a partially depleted operation, respectively. Therefore, there exists a field-free substrate region for the filled-circle data alone. The origin of the abscissa is defined at the location of the incident-beam edge; that is, an additional scan of  $y = 0.5 \mu\text{m}$  or  $\theta = 0.005^\circ$  makes a signal output for the adjoining channel to the channel located at the beam edge in a fully depleted operation [Fig. 4(a)].

The curves in Fig. 4(b) stand for the calculated diffusion signals  $I_{\text{dif}}$  for detector channels aligned in the  $y$  direction using our three-dimensional diffusion theory [see Eq. (9)]. Here we utilize three values of the three-dimensional charge diffusion length  $L$  of 50 (dashed curve), 100 (solid curve), and  $150 \mu\text{m}$  (dotted curve) for fitting the spatially diffusing charge profile produced at the 9.5-keV monoenergy photons.

The diffusion signal is clearly observed when the applied bias is reduced and the field-free substrate region is formed. The charges created by the incident photons diffuse three dimensionally in the field-free substrate region, while the charges produced in the depletion layer drift along the electric field one dimensionally without the penetration into the adjoining channels.

It is important to note that the shape of the charge-diffusion distribution from the substrate to the bottom surface of the depletion layer is maintained because of the one-dimensional quick drift through the depletion layer to the electrode. Therefore, the output diffusion signals from the electrode directly indicate the diffusion distribution at the bottom surface of the depletion layer, as calculated in Sec. II. It is again noted that the charges produced in the depletion layer do not contribute to these diffusion signals in the neighboring channels separating from the x-ray incident channel. This important mechanism will play an essential role in our proposed method in Sec. V.

In addition to these data on  $L$  using the distribution shape, the values of  $d_{\text{dep}}$  are measured using a computer-controlled capacitance detector as a function of an applied voltage (a  $C$ - $V$  characterizer); this standard method for identifying  $d_{\text{dep}}$  provides us with useful information on one of the two free parameters (i.e.,  $L$  and  $d_{\text{dep}}$ ) in our theoretical predictions of the photon energy responses of semiconductor detectors.

The data on the photon energy response are compared to the predicted response in Eq. (5) using the observed values of  $L$  and  $d_{\text{dep}}$  along with the other detector parameters in Eq. (5). The validity of the theory is verified by the energy response data using the same method as in Refs. [2, 17].

Thus we have constructed and verified the theory. We now proceed to develop the theory into a proposal of an alternative method for  $T_e$  measurements (see Sec. V) so as to clarify the physics principle through such examples of application.

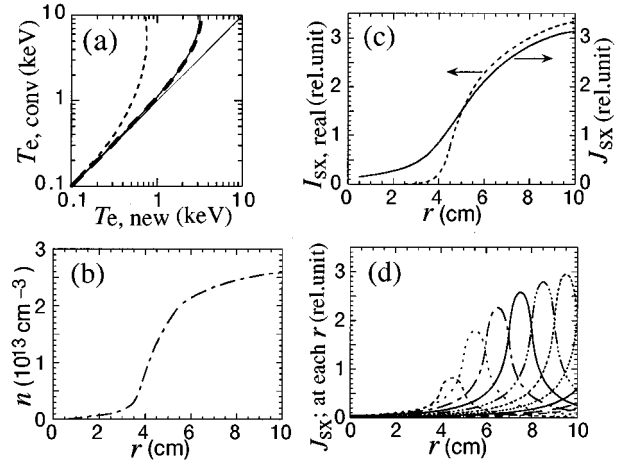


FIG. 5. (a) Difference between the actual plasma electron temperatures  $T_{e,\text{new}}$  obtained by our theory using Eq. (5) (or from synchrotron-radiation experiments) and the commonly estimated temperatures  $T_{e,\text{conv}}$  from the conventional theory [4]. The cases of  $d_{\text{dep}} = 10, 10, \text{ and } 1 \mu\text{m}$  along with  $L = 100 \mu\text{m}$ ,  $d_{\text{dead}} = 0.1 \mu\text{m}$ ,  $d_{\text{sub}} = 300 \mu\text{m}$  are represented by the solid, dashed, and dotted curves, respectively; for the case of the dashed curve, a 1800-Å-thick Al window is also attached. (b) Example of the density profile in an  $H$  mode. (c) Predicted detector signals  $J_{sx}$  (solid curve) from our theory [see Eq. (5)] compared to the actual x-ray profile  $I_{sx,\text{real}}$  (dashed curve) (see Ref. [19]) estimated from the data on the density in (b). (d) Charge-diffusion distributions at several radii calculated using Eq. (8); the summation of the overlap of these charge-diffusion distributions forms a broader profile [the solid curve in (c)] as compared to the actual profile [the dashed curve in (c)]. Here the values of  $d_{\text{sub}} = 300 \mu\text{m}$  and  $L = 100 \mu\text{m}$  are utilized.

### IV. EFFECTS OF THE PROPOSED THEORY ON THE ANALYSES OF PLASMA X-RAY DATA AND THEIR INTERPRETATIONS

Recently, underbiased operations of multichannel semiconductor detectors have been employed widely in various plasma devices including the JET [8], the DIII-D [6], and the ASDEX Upgrade [9] tokamaks in order to avoid detector breakdown caused by intense x-ray or neutron influxes. In such a partially depleted detector operation, the above-described diffusion effect becomes essentially of importance for x-ray data analyses since the energy response of such a detector changes according to whether or not the diffusion effect is taken into account.

As discussed in Sec. II for a single-channel semiconductor detector, the charge diffusion contributes to the enhancement of the detector signal [see Eq. (5)]. If the conventional theory [4] is employed in place of our proposed theory, then the exclusion of the diffusion effect leads to the underestimation of the energy response (i.e., the quantum efficiency) of a semiconductor detector and thereby the overcompensation of the detector response for  $T_e$  analyses as described in the following.

In Fig. 5(a), actual plasma electron temperatures  $T_{e,\text{new}}$  using Eq. (5) from our theory on the detector response (or from synchrotron-radiation data) are compared to those using the commonly utilized conventional theory  $T_{e,\text{conv}}$ . Here x-ray energy spectra are calculated using emission from relativistic Maxwellian electrons [11–14]. For the values of the

x-ray cross section, the relativistic Born approximation corrected by the Elwert factor is utilized [18–20]. The solid, dashed, and dotted curves in Fig. 5(a) stand for the cases of  $d_{\text{dep}} = 10, 10,$  and  $1 \mu\text{m}$ , respectively, along with  $L = 100 \mu\text{m}$ ; in addition, a 1800-Å-thick aluminum window is attached for the case of the dashed curve. These values are cited from the parameters of commercially available detectors. It should be noted that serious errors even for  $T_e < 1 \text{ keV}$  occur when widely utilized underbiased operations are employed. A greater overestimation is predicted to occur with the application of the conventional theory to analyze x rays from higher-temperature plasmas since higher-energy x rays penetrating through a depletion layer and deeply into a field-free substrate region enhance the diffusion effect in the substrate region for the total signal. This is the reason high- $T_e$  devices including JET [8], DIII-D [6,21], and ASDEX Upgrade [21,22] have recently employed our theory.

Furthermore, one should cautiously interpret the plasma x-ray tomography data using multichannel semiconductor detectors. Figure 5(b) shows one of the typical profiles of plasma density  $n$ , characterized by a steep gradient in a peripheral plasma region as typically observed in a H mode or a very H mode. The abscissa indicates the plasma minor radius  $r$ . The profile of the actual x-ray emissivity (proportional to  $n^2 T_e^{1/2}$ ) is estimated as the dashed curve in Fig. 5(c), where  $T_e$  is approximated to be a flat profile for highlighting the effect of  $n$ .

On the other hand, the curves in Fig. 5(d) show the charge-diffusion profiles at several radial positions calculated from the real x-ray profile  $I_{\text{sx,real}}$  [the dashed curve in Fig. 5(c)] using our diffusion theory under the partially depleted operational conditions. The three-dimensional charge-diffusion effect modifies the detector output signals due to the charges diffusing into the neighboring detector channels as seen in Fig. 5(d). A spurious x-ray profile caused by these diffusing charges is calculated from the summation of the charges diffusing from each x-ray-injection location of  $r$ , as depicted in Fig. 5(d). A resultant broader profile shown as the solid curve in Fig. 5(c) highlights a misinterpretation of the real narrower x-ray profile plotted as the dashed curve in Fig. 5(c). In Figs. 5(c) and 5(d), we employ a photon energy of 1.8 keV as a representative value of  $T_e$  of the order of keV.

The appearance of plasma peaking profiles in various types of high-confinement modes enhances the importance of the present studies for plasma x-ray diagnostics, since the diffusion significantly deforms the real gradients of the plasma parameters, and affects the estimation of electron-energy transport, bootstrap currents, and so on. In JET, careful experimental studies of such channel cross talk effects are in fact reported [8]. A 10% channel cross talk (expected to be dependent on the incident x-ray energy) is observed in the x-ray-detector signals.

## V. PROPOSED METHOD FOR PLASMA ELECTRON-TEMPERATURE DIAGNOSTICS ON THE BASIS OF THE ABOVE-VERIFIED PRINCIPLE

### A. Proposed principle of x-ray data analyses for $T_e$ measurements using the three-dimensional diffusion effects

In Sec. IV, the serious effects of charge diffusion on signal analyses were investigated. Such effects seem to discour-

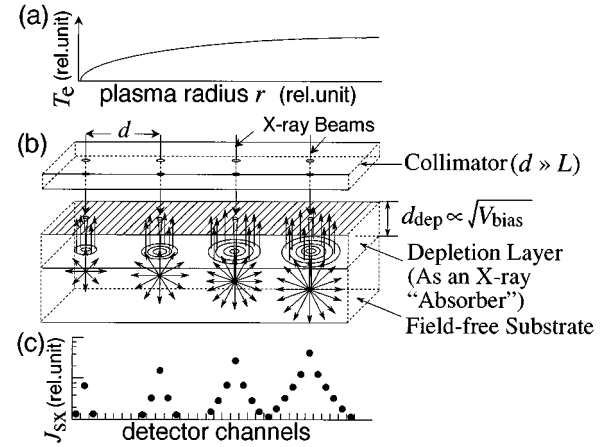


FIG. 6. Schematic view of the proposed x-ray analysis method for  $T_e$  observations using our proposed physical mechanisms in a semiconductor x-ray detector. X rays from plasmas with a  $T_e$  profile in (a) are incident onto a multichannel semiconductor-detector array with several collimator apertures in (b) so as to obtain charge-diffusion signal distributions  $J_{\text{sx}}$  in (c). These distributions are fitted by our theoretically predicted curves (see Fig. 8). Here the apertures are located under the condition of  $d \gg L$  for no overlapping of the diffusion distributions. Note that the depletion layer (having no three-dimensional charge diffusion into the neighboring channels) plays the role of an x-ray ‘‘absorber’’ for the diffusion charges, which are produced in the field-free substrate and then flow into the neighboring channels. The value of  $d_{\text{dep}}$  (i.e., the thickness of the absorber of x rays; x rays penetrated into the substrate play the role of the source of the charge diffusion into the neighboring channels) is externally controllable by means of variation in  $V_{\text{bias}}$  because of  $d_{\text{dep}} \propto V_{\text{bias}}^{1/2}$ .

age the conventional x-ray tomography diagnostics using widely utilized multichannel semiconductor detectors because of complicated problems including channel cross talks.

However, in order to overcome such serious situations, in this section, we propose an alternative x-ray diagnostic method for  $T_e$  measurements on the basis of our theory (Sec. II) on semiconductor-detector responses. This proposal using the three-dimensional diffusion replaces the serious effect of the diffusion [Figs. 5(a) and 5(c)] by a useful theory. The theory is based on the dependence of the charge-diffusion distribution on  $E$  [Fig. 2(b)]. In addition, the present example of the use of the above-verified theory (Sec. IV) may help clarify the method.

First we prepare a multichannel semiconductor-detector array as illustrated in Figs. 2 and 6; each channel width of a few tens of micrometers is sufficiently shorter than the diffusion length  $L$ . Such a multichannel detector is commercially available in standard stock. The detector is covered with a collimator having several apertures in order to observe x rays from several plasma radii [Fig. 6(a)]. Each aperture locates in line at intervals of  $d$  under the condition  $d \gg L$  [Fig. 6(b)] so as not to overlap each charge-diffusion distribution produced by transmitted x rays through each aperture. The charge-diffusion distributions are then obtained as illustrated in Fig. 6(c).

On the other hand, the diffusing charges distribute to the detector channels adjoining each x-ray incident channel ac-

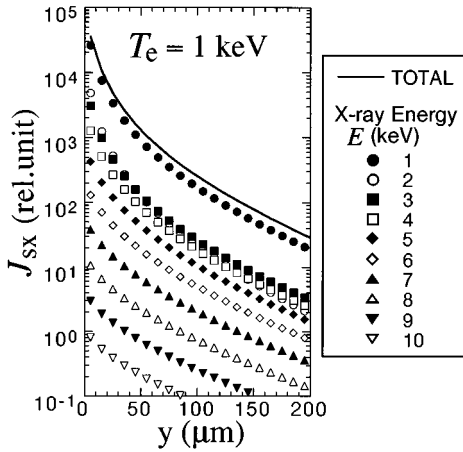


FIG. 7. Charge-diffusion distributions produced by several monoenergetic x rays (see various marks in the figure) emitted from 1-keV Maxwellian plasmas, calculated from Eq. (8) with  $L = 100 \mu\text{m}$  and  $d_{\text{sub}} = 300 \mu\text{m}$ . Here x rays are injected into the detector at  $y = 0$ . The summation of each signal distribution is plotted by the solid curve.

According to the dependence on the incident x-ray energy [Fig. 2(b)]; that is, both the charge-production depth and the amount of charges produced in the field-free substrate depend on x-ray energies. Thus the resultant slope of the charge-diffusion distribution gives information on the incident x-ray energy. This slope itself is independent of the plasma density since the density modifies only the incident x-ray intensities. If the temporal evolution of the plasma densities is slower than the time for the charge diffusion (of the order of microseconds), then such a density variation provides no effects on the slope of the charge-diffusion distribution [see Fig. 2(b)].

On the other hand, the dependence of the charge-diffusion distribution on  $T_e$  is investigated as follows. In Fig. 7, the solid curve stands for the total charge-diffusion distribution resulting from the summation of the distributions produced by incident x rays with various energies at  $x = y = 0$ . Here x rays are emitted from Maxwellian plasmas with  $T_e = 1 \text{ keV}$ . For simplicity, no absorption effects in the dead layer and the depletion layer are assumed (for more details, see below) and  $d_{\text{sub}} = 300 \mu\text{m} = 3L$  is employed for a sufficient amount of x-ray absorption in this energy range.

Similarly, the total diffusion distributions with various  $T_e$  are depicted in Fig. 8. The solid, dashed, dotted, and dot-dashed curves correspond to  $T_e = 1, 2, 3,$  and  $5 \text{ keV}$ , respectively. For comparison, in Fig. 8(a), the values of the distributed charges  $J_{sx}$  are calculated for a constant plasma density, while the values of  $J_{sx}$  in Fig. 8(b) are normalized by the charges at  $y = 0$  to highlight the difference in the distribution slopes labeled with various  $T_e$ . Here the typical values of  $L = 100 \mu\text{m}$ ,  $d_{\text{sub}} = 300 \mu\text{m}$ , and  $d_{\text{dep}} = 5 \mu\text{m}$  in a partially depleted operation are utilized.

It is again noted that these distributions are formed within a diffusion time of the order of microseconds; thus plasmas in a quasisteady state during that diffusion time are sufficient for the use of this proposed method for  $T_e$  analyses. Such a

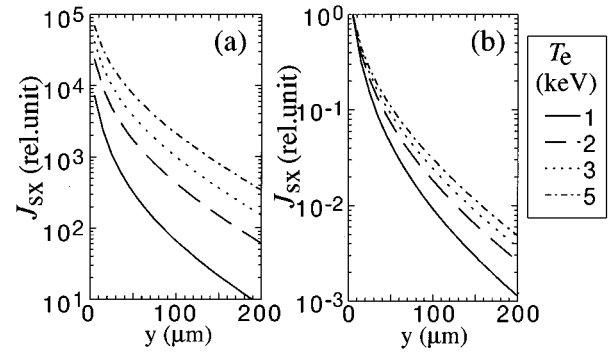


FIG. 8. (a) Charge-diffusion distributions produced by x rays from normalized plasma densities, depicted for  $T_e = 1, 2, 3,$  and  $5 \text{ keV}$  plasmas as the solid, dashed, dotted, and dot-dashed curves, respectively. (b) For comparison, the diffusion distributions in (a) are normalized by the signal outputs at  $y = 0$ . These calculated distributions as a function of  $T_e$  provide a set of the “distribution-analysis” bases so as to obtain  $T_e$  using the proposed alternative x-ray analysis principle. Here the parameters  $L = 100 \mu\text{m}$ ,  $d_{\text{sub}} = 300 \mu\text{m}$ , and  $d_{\text{dep}} = 5 \mu\text{m}$  are employed.

time scale may be acceptable for most macroscopic plasma behavior in various types of plasma confinement devices. These calculated results of charge-diffusion distributions as a function of  $T_e$  provide a set of “distribution analysis” bases for fitting the charge-diffusion distributions [Fig. 6(c)] so as to obtain  $T_e$  easily.

The characteristic features of our proposal to observe  $T_e$  indicate striking differences compared with the conventional methods using direct observations of x-ray bremsstrahlung for  $T_e$  analyses. As described above, our proposed method for  $T_e$  measurements has no dependence on  $n$ ; this characteristic property solves a complicated problem of the conventional x-ray analysis method, which has a functional dependence on both  $n$  and  $T_e$ .

### B. Alternative method on the basis of the proposed theory in $T_e$ measurements using a single plasma shot

The proposed theory in Sec. V A is exemplified in this subsection for  $T_e$  measurements using a single plasma shot only. This would also provide a further detailed picture of the proposed physics principle.

For comparison with the standard methods of plasma x-ray diagnostics, we briefly characterize the following two standard methods. For the x-ray-absorption method using various x-ray-absorption filters [10], the depletion layer is utilized as the x-ray-sensitive detection region [4] using shot-to-shot variation in an x-ray-absorber thickness or an absorber material. The dependence of the x-ray-detector signals on the absorber is employed according to well-established calculation curves [10–13] as a function of an x-ray-absorber thickness (thereby being widely referred to as the x-ray-absorption method). The absorption method in a pileup current mode and the x-ray PHA method in an x-ray-produced pulse-counting mode without pileup signals are two typical x-ray analysis methods.

The former has the following merits. X-ray collimation does not require an observation limit to x-ray intensities because of its intrinsic property as a pileup mode; this makes x-ray tomography diagnostics possible without changing the apertures under the conditions of a significant variation in x-ray intensities at various plasma radii as well as at several types of discharges with a wide dynamic range from low to high  $T_e$ . Even under these conditions, with considerable intensity variations, it is not necessary for a current mode to change an x-ray system located in a vacuum chamber. A problem for  $T_e$  measurements, however, exists in its signal dependence on complicated plasma parameters including  $T_e$  and  $n$  as described above.

On the other hand, the latter method is useful in obtaining x-ray energy spectra directly, although there are several problems including the necessity of summing up many plasma shot data or a long duration for x-ray pulse sampling in order to attain a sufficient number of x-ray pulse signals for a spectrum formation. Another requirement is the adjustment of x-ray collimation so as to avoid the pileup of x-ray pulse signals. This problem is serious for a shot, in which  $T_e$  or  $n$  changes significantly, or for an experimental series with a variation of plasma parameters. Furthermore, in actual observations, the x-ray PHA method is not available when tomographically reconstructed analyses are required since a huge amount of data and complicated reconstructions are necessary to obtain actual x-ray spectra at various plasma radii.

In order to alternate these two standard x-ray diagnostic methods, a third method for x-ray analyses is proposed in this article using a different theory from those in the above two standard methods. The essential point of the proposal is based on the use of a depletion layer covering over a field-free substrate as a temporally variable x-ray absorber within one plasma shot. For the observations of three-dimensional charge-diffusion distributions, output-signal charges produced directly in the depletion layer of the incident x-ray channel give no contribution to the neighboring-channel output since a strong electric field in the depletion layer sweeps the produced charges one dimensionally directly into its own channel electrode. Such a ‘‘direct’’ signal from a depletion layer is widely utilized for the above two standard methods as an output signal. However, for our proposed method, such a depletion layer is utilized as an externally controllable x-ray absorber for the production of the charge-diffusion signals in the substrate located below the depletion layer. In particular, it is noted that such an absorber thickness is proportional to the square root of an externally applied bias voltage  $V_{\text{bias}}$ . Thus a large value of  $V_{\text{bias}}$  results in a ‘‘thick x-ray absorber’’ in front of the diffusion signal production region since incident x rays are absorbed in the thick depletion layer and then the charges produced there do not contribute to three-dimensionally diffusing charges into the neighboring channels. Therefore, the temporal variation in  $V_{\text{bias}}$ , controlled externally during one plasma shot, corresponds to the temporal change in the x-ray-absorber thickness during a shot. No changes in real absorber materials are required for changing the x-ray energy range to carry out this ‘‘absorption method.’’

This proposed principle is extended to be exemplified by the use of commercially available multichannel detectors. In

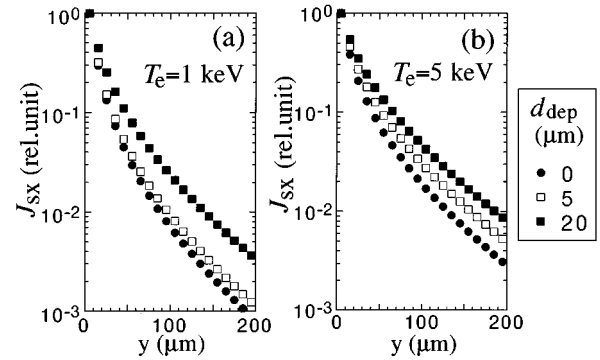


FIG. 9. Charge-diffusion distributions for  $T_e$  of (a) 1 and (b) 5 keV. These are calculated using the depletion-layer thicknesses of  $d_{\text{dep}}=0, 5,$  and  $20 \mu\text{m}$  and are plotted by the filled circles, open squares, and filled squares, respectively. Here  $L=100 \mu\text{m}$  and  $d_{\text{sub}}=300 \mu\text{m}$  are utilized.

Figs. 9(a) and 9(b), the charge-diffusion distributions are calculated using various depletion-layer absorber thicknesses of  $d_{\text{dep}}=0, 5,$  and  $20 \mu\text{m}$  and the results are normalized by the signal outputs at  $y=0$  for  $T_e=1$  and 5 keV, respectively. Here x rays are injected into the detector with  $d_{\text{sub}}=300 \mu\text{m}$  at  $-10 \mu\text{m}<y<0$  in the form of a pencil beam. As seen in Figs. 9(a) and 9(b), not only the difference in the distributions between  $T_e=1$  and 5 keV for the same value of  $d_{\text{dep}}$ , but also their dependence on  $d_{\text{dep}}$  even for the same value of  $T_e$  is clearly shown.

Furthermore, one of the easier and convenient realizations of the proposed third alternative principle is as follows. Figure 10(a) shows the dependence of the total charge-diffusion outputs integrated over all neighboring channels on the variation in  $d_{\text{dep}}$  (or, equivalently, in the detector applied bias). For each curve labeled with a constant value of  $T_e$ , the output signal  $J_{sx}$  is normalized by that at  $d_{\text{dep}}=0$ . The same conditions of x-ray incidence are employed as in Fig. 9. Figure 10 is prepared for the convenience of researchers who utilize only two-channel detectors (i.e., for x-ray injection into one channel, the output signals being observed from another neighboring channel under the condition of a channel width wider than a few times  $L$  for collecting all diffusing charges) or who require a better signal-to-noise ratio even in the case with lower  $T_e$ .

From this viewpoint, the integration over all diffusion charges plotted at  $y>0$  in Fig. 9 for a set of the selected values of  $T_e$  and  $d_{\text{dep}}$  (or  $V_{\text{bias}}$ ) provides one corresponding point on a curve in Fig. 10(a) (i.e., the point having the above-selected value of  $d_{\text{dep}}$  on the curve labeled with the selected value of  $T_e$ ). Suppose that the case of  $T_e=1$  keV, for instance, an integrated value over all  $J_{sx}$  plotted as open squares in Fig. 9(a), results in a value of  $J_{sx}$  at  $d_{\text{dep}}=5 \mu\text{m}$  on the curve labeled with  $T_e=1$  keV in Fig. 10(a). Similarly, the curves in Fig. 10 are easily calculated using the basic data in Fig. 9 for any value of  $T_e$ . As we see in Fig. 10(a), a scan of  $d_{\text{dep}}$  (by means of variation in the externally applied detector bias) draws a clearly distinguishable curve for a value of  $T_e$ ; thus such a characteristic feature demonstrates the practical applicability of the proposed third alternative



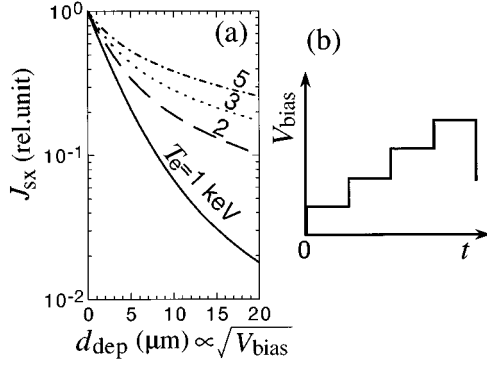


FIG. 10. (a) Dependence of the charge-diffusion outputs on the depletion-layer thicknesses (being equivalent to the detector applied biases) for  $T_e=1, 2, 3,$  and  $5$  keV, shown by the solid, dashed, dotted, and dot-dashed curves, respectively. In contrast to the widely utilized x-ray observation methods including the x-ray-absorption method and the x-ray PHA, a depletion layer is utilized in our proposed method as an x-ray absorber for the charge diffusion produced below the depletion layer (i.e., in the field-free substrate). The integration over all charge diffusion at  $y>0$  (see Fig. 9) is carried out for practical convenience using a two-channel detector; that is, x rays are incident onto one channel and then the diffusion signals are taken from another neighboring channel. Here a channel width (sufficiently wider than a few times  $L$ ) is required for all charge collections (for more details, see the text). (b) Multiple-step-shaped biasing during one plasma shot with constant-voltage durations of the order of the charge-diffusion time, exemplified so as to obtain the temporal evolution of  $T_e$  using one plasma shot only; here, the dependence of the charge-diffusion outputs on the depletion-layer thickness in (a) is usefully employed. One cycle for the multiple-step biasing requires, for instance, of the order of  $100 \mu\text{s}$  for attaining ten data points to fit a curve in (a). These examples would provide further understanding of our proposed theory.

x-ray diagnostic method for  $T_e$  measurements as an example of the use of the above-described theory.

It is also noted that the proposed method is useful when impurity line radiation exists. If we sweep  $V_{bias}$  slowly and carefully and if  $d_{dep}$  becomes thicker than the characteristic value  $d_L$ , then we may obtain a significant charge in the output signal. Here the value of  $d_L$  satisfies the relation of  $d_L=1/[\mu(E_L)\rho]$ . When  $d_{dep}$  becomes thicker than the critical characteristic thickness of  $d_L$ , the line radiation having a narrow spectrum peaked at  $E=E_L$  is absorbed exponentially and reduced significantly as compared to bremsstrahlung having a much broader spectrum even beyond  $E_L$ . Such freely adjustable filtering of impurity lines is difficult for the conventional absorption filter method since such a change in the filter material thickness during a plasma shot is not practical. Also, it is difficult to provide various filter material thicknesses corresponding to various impurity lines by the use of a limited space for absorbers. The method for varying and optimizing the absorber thickness  $d_{dep}$  by means of detailed external bias control is one of the characteristic merits of identifying and distinguishing the existence of line radiation using the present method on the basis of the proposed theory.

As one method of the practical applications of the above x-ray diagnostic principle, we propose a special form of bi-

asing for an easier realization of this idea. A step-shaped biasing with multiple discrete values during one biasing cycle is proposed to be supplied to the detector [Fig. 10(b)]. Each flat value of  $V_{bias}$  corresponding to each value of  $d_{dep}$  ( $d_{dep}\propto V_{bias}^{1/2}$ ) should be maintained during the characteristic time of the charge diffusion. Following the formation of a quasisteady distribution of such diffusion charges, a data sampling is then carried out. Similarly, the next step biasing provides another data point. After one biasing cycle, a data set for fitting the curves in Fig. 10(a) is then completed. An estimated cycle of the multistep biasing is, for instance, of the order of  $100 \mu\text{s}$  for ten data points; therefore, this method is applicable to plasmas having a quasisteady state with the duration of  $100 \mu\text{s}$  for every data set of ten points. Such a quasisteady time scale required for the proposed x-ray diagnostic method of  $T_e$  measurements may be satisfied with various physics phenomena in various types of plasma-confinement devices.

The proposed physics principle in this article would begin to open possibilities for analyzing and interpreting plasma-physics frontier phenomena, which have not been addressed or clarified using the conventional x-ray diagnostics in a single plasma shot.

## VI. SUMMARY

An alternative physics principle and method for x-ray diagnostics is proposed in this article to obtain plasma electron temperatures and behavior. This (Sec. II) is different from the widely utilized standard methods of x-ray-absorption method with various x-ray filters and of x-ray pulse-height analysis. The theory for the proposed method is directly verified by data on distributions of three-dimensionally diffusing charges (Sec. III) in synchrotron-radiation experiments. Such a direct verification of the theory predicts the overestimation of electron temperatures, when the conventional theory [4], utilized over this quarter of the century, is employed [Fig. 5(a)].

Our theory also predicts the channel cross talk for a multichannel semiconductor detector, which was experimentally reported by careful works in the JET tokamak [8]. Such an effect results in the misunderstanding of broader plasma profiles compared to actual ones [Fig. 5(c)]. This leads to the misestimation of the gradients of plasma temperatures or pressures, resulting in misinterpretation of pedestal structures in H modes, electron-energy transport, as well as the misestimation of bootstrap currents and hence the misinterpretations of plasma physics (Sec. IV).

An alternative method on the basis of the above x-ray diagnostic principle is proposed for the purpose of actual  $T_e$  analyses. This method employs the depletion layer of a semiconductor detector as an externally changeable x-ray absorber during one plasma shot in place of its standard use as an x-ray-sensitive region. A basic idea of the alteration using a multichannel detector is illustrated in Fig. 6 and is exemplified in Figs. 7–9 (Sec. V) so as to clarify the proposed theory. In addition, a convenient example is proposed using a temporally varying multiple-step-shaped biasing in Fig. 10(b) for a simple two-channel detector; this would analyze

the temporal evolution of  $T_e$  with a cyclic period of the order of 100  $\mu\text{s}$  (Sec. V B).

The proposed theory in x-ray diagnostics described in this article therefore provides not only precise fundamentals for plasma-physics analyses using x rays (Secs. II and III) but also practical alternative methods using a simple x-ray diagnostic system (Sec. V) as well as the actual understandings of the observed x-ray signals for the interpretations of plasma physics (Sec. IV).

#### ACKNOWLEDGMENTS

The authors would like to acknowledge the members of the GAMMA 10 Group for their collaboration and the members of the National Institute for High Energy Physics for their useful discussions. Financial support of this work was partly afforded by a Grant-in-Aid for Science Research from the Ministry of Education, Science and Culture of Japan. J.K. was supported by the Japan Society for the Promotion of Science.

- 
- [1] T. Cho *et al.*, Nucl. Instrum. Methods Phys. Res. A **348**, 475 (1994).
- [2] T. Cho *et al.*, Phys. Rev. A **46**, 3024 (1992).
- [3] T. Cho *et al.*, J. Appl. Phys. **72**, 3363 (1992).
- [4] W. J. Price, *Nuclear Radiation Detection* (McGraw-Hill, New York, 1964), Chap. 8.
- [5] S. von Goeler *et al.*, Phys. Rev. Lett. **33**, 1201 (1974).
- [6] R. T. Snider, Nucl. Fusion **30**, 2400 (1990); Rev. Sci. Instrum. **66**, 546 (1995).
- [7] R. D. Gill, Nucl. Fusion **29**, 397 (1989).
- [8] B. Alper, S. Dillon, A. W. Edwards, R. D. Gill, R. Robins, and D. J. Wilson, Rev. Sci. Instrum. **68**, 778 (1997).
- [9] M. Bessenrodt-Weberpals, J. C. Fuchs, M. Sokoll, and the ASDEX Upgrade Team, IPP Report No. IPP 1/290, 1995 (unpublished).
- [10] F. C. Jahoda *et al.*, Phys. Rev. **119**, 843 (1960).
- [11] T. Cho *et al.*, Phys. Rev. Lett. **64**, 1373 (1990).
- [12] T. Cho *et al.*, Phys. Rev. A **45**, 2532 (1992).
- [13] T. Cho *et al.*, Nucl. Fusion **27**, 1421 (1987).
- [14] M. Hirata *et al.*, Jpn. J. Appl. Phys. **28**, 96 (1989).
- [15] J. Kohagura *et al.*, Rev. Sci. Instrum. **66**, 2317 (1995).
- [16] J. Kohagura *et al.*, Appl. Radiat. Isot. **46**, 489 (1995).
- [17] T. Cho *et al.*, Rev. Sci. Instrum. **66**, 543 (1995).
- [18] H. Bethe and W. Heitler, Proc. R. Soc. London, Ser. A **146**, 83 (1934).
- [19] R. L. Gluckstern, M. H. Hull, Jr., and G. Breit, Phys. Rev. **90**, 1026 (1953); **90**, 1030 (1953).
- [20] G. Elwert, Ann. Phys. (Leipzig) **34**, 178 (1939).
- [21] T. Cho *et al.*, in *Proceedings of the International Conference on Plasma Physics*, Nagoya, 1996, edited by H. Sugai and T. Hayashi (The Japan Society of Plasma Science and Nuclear Fusion Research, Nagoya, 1996), Vol. 2, p. 1486.
- [22] T. Cho *et al.*, Rev. Sci. Instrum. **68**, 774 (1997).